LA-14219
Issued: May 2005

Off-Beam Cloud Lidar: A New Diffusion Model and a Comparison with LITE Returns

Igor N. Polonsky
Anthony B. Davis

Los Alamos NATIONAL LABORATORY EST. 1943

The World's Greatest Science Protecting America

Off-Beam Cloud Lidar:
A New Diffusion Model and
a Comparison with LITE Returns
by

Igor N. Polonsky and Anthony B. Davis

Los Alamos National Laboratory

Space and Remote Sensing Sciences Group (ISR-2)

Los Alamos, NM 87545, USA

Abstract

In the paper the diffusion approximation solution in the time and spatial domain is discussed with regard to the active cloud probing. This solution can be used as a base for a retrieval technique which was demonstrated by developing a space lidar data (the LITE campaign). The obtained results were compared with one retrieved by a Monte-Carlo based technique showing a good accuracy.

1. Space- and/or time-domain Green functions in the diffusion limit

Consider a homogeneous slab of a scattering and weakly absorbing medium of geometrical thickness H and optical thickness τ_H illuminated by a collimated/pulsed laser beam normal to the boundary plane. This problem can be reduced via Fourier in 2D space and Laplace in time transforms to the classic problem of uniform/steady illumination at normal incidence [1]. So we can use the reflection function

$$R = \int\limits_{\mu<0} I(z, \vec{r}, \vec{n})|\mu|\mathrm{d}\vec{n} \tag{1}$$

for the flux from such a slab in the steady state and 1D case may be written in the following form [2]

$$R = \frac{\sinh[m(H-q)]}{\sinh[m(H+4q)]}, \tag{2}$$

which is accurate up to order m^2. Here, we have defined

$$q = \frac{1}{3(s+\sigma-\sigma_{\mathrm{s}}g)}, \tag{3}$$

$$m = \sqrt{k^2+\gamma^2}, \tag{4}$$

$$\gamma = \sqrt{3(s+\sigma-\sigma_{\mathrm{s}})(s+\sigma-\sigma_{\mathrm{s}}g)} \tag{5}$$

where g is the asymmetry factor of the phase function, σ and σ_{s} are the extinction and scattering coefficients, respectively; $\vec{k}$ is image variable for the Fourier transform with respect to the 2D vector $\vec{r} = (x, y)$; and s is the image variable for the Laplace transformation with respect to time t.

We first transform Eq. (2) to an equivalent but more convenient form for usage further on

$$R = \sum_{n=0}^{\infty} \{\exp\left[-m(2nY+X)\right] - \exp\left[-m(2[n+1]Y-X)\right]\} \tag{6}$$

where

$$Y = H + 4q, \tag{7}$$

$$X = 5q. \tag{8}$$

Now we apply the inverse Fourier transform, considering that

$$R(...,\vec{r},...)=\frac{1}{4\pi^2}\int\int R(...,\vec{k},...)\exp(\ \vec{r}\cdot\vec{k})\mathrm{d}\vec{k}, \tag{9}$$

$$R(...,r,...)=\frac{1}{2\pi}\int\limits_0^\infty R(...,k,...)J_0(rk)k\mathrm{d}k, \tag{10}$$

and

$$\mathrm{e}^{-a\sqrt{k^2+b^2}}=-\frac{\mathrm{d}}{\mathrm{d}a}\frac{\mathrm{e}^{-a\sqrt{k^2+b^2}}}{\sqrt{k^2+b^2}}, \tag{11}$$

$$\int\limits_0^\infty\frac{\mathrm{e}^{-a\sqrt{k^2+b^2}}}{\sqrt{k^2+b^2}}J_0(rk)k\mathrm{d}k=\frac{\mathrm{e}^{-b\sqrt{r^2+a^2}}}{\sqrt{r^2+a^2}}, \tag{12}$$

$$\int\limits_0^\infty\mathrm{e}^{-a\sqrt{k^2+b^2}}J_0(rk)k\mathrm{d}k=\frac{a\mathrm{e}^{-b\sqrt{r^2+a^2}}}{r^2+a^2}\left[b+\frac{1}{\sqrt{r^2+a^2}}\right]. \tag{13}$$

As a result, we obtain

$$R=\sum_{n=0}^{\infty}\left\{\frac{(2nY+X)\mathrm{e}^{-\gamma\sqrt{r^2+(2nY+X)^2}}}{r^2+(2nY+X)^2}\left[\gamma+\frac{1}{\sqrt{r^2+(2nY+X)^2}}\right]\right. \tag{14}$$

$$\left.-\frac{(2[n+1]Y-X)\mathrm{e}^{-\gamma\sqrt{r^2+(2[n+1]Y-X)^2}}}{r^2+(2[n+1]Y-X)^2}\left[\gamma+\frac{1}{\sqrt{r^2+(2[n+1]Y-X)^2}}\right]\right\}. \tag{15}$$

Noticing that

$$\sum_{n=0}^{\infty}\frac{(2[n+1]Y-X)\mathrm{e}^{-\gamma\sqrt{r^2+(2[n+1]Y-X)^2}}}{r^2+(2[n+1]Y-X)^2}\left[\gamma+\frac{1}{\sqrt{r^2+(2[n+1]Y-X)^2}}\right]$$
$$=\sum_{n=1}^{\infty}\frac{(2nY+X)\mathrm{e}^{-\gamma\sqrt{r^2+(2nY+X)^2}}}{r^2+(2nY+X)^2}\left[\gamma+\frac{1}{\sqrt{r^2+(2nY+X)^2}}\right], \tag{16}$$

we arrive to a simpler form

$$R=\sum_{n=-\infty}^{\infty}\frac{(2nY+X)\mathrm{e}^{-\gamma\sqrt{r^2+(2nY+X)^2}}}{r^2+(2nY+X)^2}\left[\gamma+\frac{1}{\sqrt{r^2+(2nY+X)^2}}\right]$$
$$=-\sum_{n=-\infty}^{\infty}\frac{(2nY+X)}{r}\frac{\mathrm{d}}{\mathrm{d}r}\frac{\mathrm{e}^{-\gamma\sqrt{r^2+(2nY+X)^2}}}{\sqrt{r^2+(2nY+X)^2}}. \tag{17}$$

In turn, we now the take the inverse Laplace transformation. Assuming $s \to 0$, we have

$$q = \frac{1}{3(\sigma - \sigma_{\rm s} g)}, \tag{18}$$

$$\gamma = \sqrt{(s + \sigma - \sigma_{\rm s})/q} \tag{19}$$

and

$$R(..., t, ...) = \int\limits_{c-\mathrm{i}\infty}^{c+\mathrm{i}\infty} R(..., s, ...)\mathrm{e}^{st}\mathrm{d}s = -\mathrm{e}^{-(\sigma-\sigma_{\rm s})t} \sum_{n=-\infty}^{\infty} \frac{(2nY + X)}{r}$$
$$\times \frac{\mathrm{d}}{\mathrm{d}r} \int\limits_{c-\mathrm{i}\infty}^{c+\mathrm{i}\infty} \frac{\exp\left[-\sqrt{\frac{s}{q}}\sqrt{r^2 + (2nY + X)^2}\right]}{\sqrt{r^2 + (2nY + X)^2}} \mathrm{e}^{st}\mathrm{d}s. \tag{20}$$

Using the Baytman's [3] tables

$$\int\limits_{c-\mathrm{i}\infty}^{c+\mathrm{i}\infty} \mathrm{e}^{-\sqrt{as}}\mathrm{e}^{st}\mathrm{d}s = \frac{1}{2}\sqrt{\frac{a}{\pi t^3}} \exp\left[-\frac{a}{4t}\right] \tag{21}$$

we arrive at

$$R(..., t, ...) = \frac{\mathrm{e}^{-(\sigma-\sigma_{\rm s})t}}{4\sqrt{\pi q^3 t^5}} \mathrm{e}^{-\frac{r^2}{4qt}} \sum_{n=-\infty}^{\infty} (2nY + X) \exp\left[-\frac{(2nY + X)^2}{4qt}\right] \tag{22}$$

or

$$R = \frac{\mathrm{e}^{-(\sigma-\sigma_{\rm s})t}}{4\sqrt{\pi q^3 t^5}} \mathrm{e}^{-\frac{r^2}{4qt}} \sum_{n=-\infty}^{\infty} (2n(H + 4q) + 5q) \exp\left[-\frac{(2n(H + 4q) + 5q)^2}{4qt}\right]. \tag{23}$$

We now apply the Poisson sum rule (see Appendix), taking into account

$$\frac{1}{\sqrt{2\pi}} \int x \exp\left[-\frac{x^2}{4qt}\right] \mathrm{e}^{\mathrm{i}x\omega}\mathrm{d}x = \mathrm{i}(2qt)^{3/2}\omega \mathrm{e}^{-qt\omega^2}. \tag{24}$$

This is results in an explicit expression for the space-time Green function

$$R = \frac{\pi \mathrm{e}^{-(\sigma-\sigma_{\rm s})t}}{t(H + 4q)^2} \mathrm{e}^{-\frac{r^2}{4qt}} \sum_{m=1}^{\infty} m \sin\left(\frac{\pi 5qm}{H + 4q}\right) \exp\left[-qt\left(\frac{\pi m}{H + 4q}\right)^2\right] \tag{25}$$

which is in essence the off-beam lidar equation. We see that at any given instant the Green function is a Gaussian in space with an increasing width at half max $2\sqrt{\ln 2qt}$ and a decreasing height or spatial integral.

Integration over r yields the time-domain Green function

$$R = \frac{2\pi q \mathrm{e}^{-(\sigma-\sigma_\mathrm{s})t}}{(H+4q)^2} \sum_{m=1}^{\infty} m \sin\left(\frac{\pi 5qm}{H+4q}\right) \exp\left[-qt\left(\frac{\pi m}{H+4q}\right)^2\right] \tag{26}$$

of interest in large-footprint lidar problems, as discussed in the next section based on LITE data. It is clear that Eqs. (23) and (25) provide the dependence of R on t. It is also obvious that the former is better when $H \to \infty$, whereas the latter is more convenient to obtain asymptotic for finite H and $t \to \infty$. Comparing the first term of the corresponding series with the second one, we can deduce that in Eq. (25) we can keep only the first term in the case of

$$t > \frac{0.12}{q}(H+4q)^2, \tag{27}$$

whereas in Eq. (23) the first term makes the most contribution if

$$t < \frac{(H+4q)(H+9q)}{q\left(5+\ln\left[\frac{H+6.5q}{2.5q}\right]\right)}. \tag{28}$$

Integration over t yields the spatial Green function

$$R = \frac{\pi}{(H+4q)^2} \sum_{m=1}^{\infty} m \sin\left(\frac{\pi 5qm}{H+4q}\right) K_0\left(\frac{\pi m r}{H+4q}\right) \tag{29}$$

of interest, for instance, in radiative smoothing problems [4] as well as the analysis of off-beam lidar data [5].

2. A more rigorous approach

At this moment our starting point is Eq. (17) which can be written in a simpler form of

$$R = -\sum_{n=-\infty}^{\infty} \frac{(2nY+X)}{r} \frac{\mathrm{d}}{\mathrm{d}r} \frac{\mathrm{e}^{-\gamma\sqrt{r^2+(2nY+X)^2}}}{.} \sqrt{r^2+(2nY+X)^2} \tag{30}$$

To make the inverse Laplace transformation we assume that

$$q = \frac{1}{3(\sigma-\sigma_\mathrm{s} g)}, \tag{31}$$

$$\gamma = \sqrt{3(\sigma+s-\sigma_\mathrm{s})(\sigma+s-\sigma_\mathrm{s} g)}. \tag{32}$$

Considering that

$$\int\limits_{c-\mathrm{i}\infty}^{c+\mathrm{i}\infty} \mathrm{e}^{-x\sqrt{s^2-\sigma_\mathrm{s}(1+g)+\sigma_\mathrm{s}^2 g}}\mathrm{e}^{st}\mathrm{d}s =$$

$$\exp\left(\sigma_\mathrm{s} t\frac{1+g}{2}\right)\left[\delta(t-x)+\sigma_\mathrm{s}\frac{1-g}{2}x\frac{I_1\left(\sigma_\mathrm{s}\frac{1-g}{2}\sqrt{t^2-x^2}\right)}{\sqrt{t^2-x^2}}\right] \quad (33)$$

and neglecting the δ-function term as nonphysical, we arrive at

$$R = -\sqrt{3}\sigma_\mathrm{s}\frac{1-g}{2}\exp\left[-t\left(\sigma+\sigma_\mathrm{s}\frac{1+g}{2}\right)\right]$$
$$\sum_{n=-\infty}^{\infty}\frac{\mathrm{d}}{\mathrm{d}(2nY+X)}\frac{I_1\left(\sigma_\mathrm{s}\frac{1-g}{2}\sqrt{t^2-3r^2-3(2nY+X)^2}\right)}{\sqrt{t^2-3r^2-3(2nY+X)^2}}. \quad (34)$$

This results in

$$R = \sqrt{27}\left[\sigma_\mathrm{s}\frac{1-g}{2}\right]^2\exp\left[-t\left(\sigma+\sigma_\mathrm{s}\frac{1+g}{2}\right)\right]$$
$$\sum_{n=-\infty}^{\infty}(2nY+X)\frac{I_2\left(\sigma_\mathrm{s}\frac{1-g}{2}\sqrt{t^2-3r^2-3(2nY+X)^2}\right)}{t^2-3r^2-3(2nY+X)^2}. \quad (35)$$

The Poisson sum rule then provides us with another form of this formula

$$R = \frac{2\pi}{\sqrt{3}Y^2\sqrt{t^2-3r^2}}\exp\left[-t\left(\sigma+\sigma_\mathrm{s}\frac{1+g}{2}\right)\right]\sum_{m=1}^{\infty}m\sin\left[\frac{\pi m X}{Y}\right]$$
$$\times\left[\cos\left(\sqrt{t^2-3r^2}\sqrt{\frac{1}{3}\left[\frac{\pi m}{Y}\right]^2-\left[\sigma_\mathrm{s}\frac{1-g}{2}\right]^2}\right)-\cos\left(\frac{\pi m}{Y}\sqrt{t^2-3r^2}\right)\right]. \quad (36)$$

3. LITE data from marine stratocumulus: Retrieval of cloud properties

All four (!) of the *unsaturated* returned pulses for LITE's [6] wide field of view (FOV) during night orbit # over an extended marine Sc deck are plotted on Fig. 1. Predictions of the diffusion approximation (DA) employing Eq. (25), taking into account the first 30 terms, are also plotted together with results using only the first terms of the summations in Eqs. (23) and (25); clearly

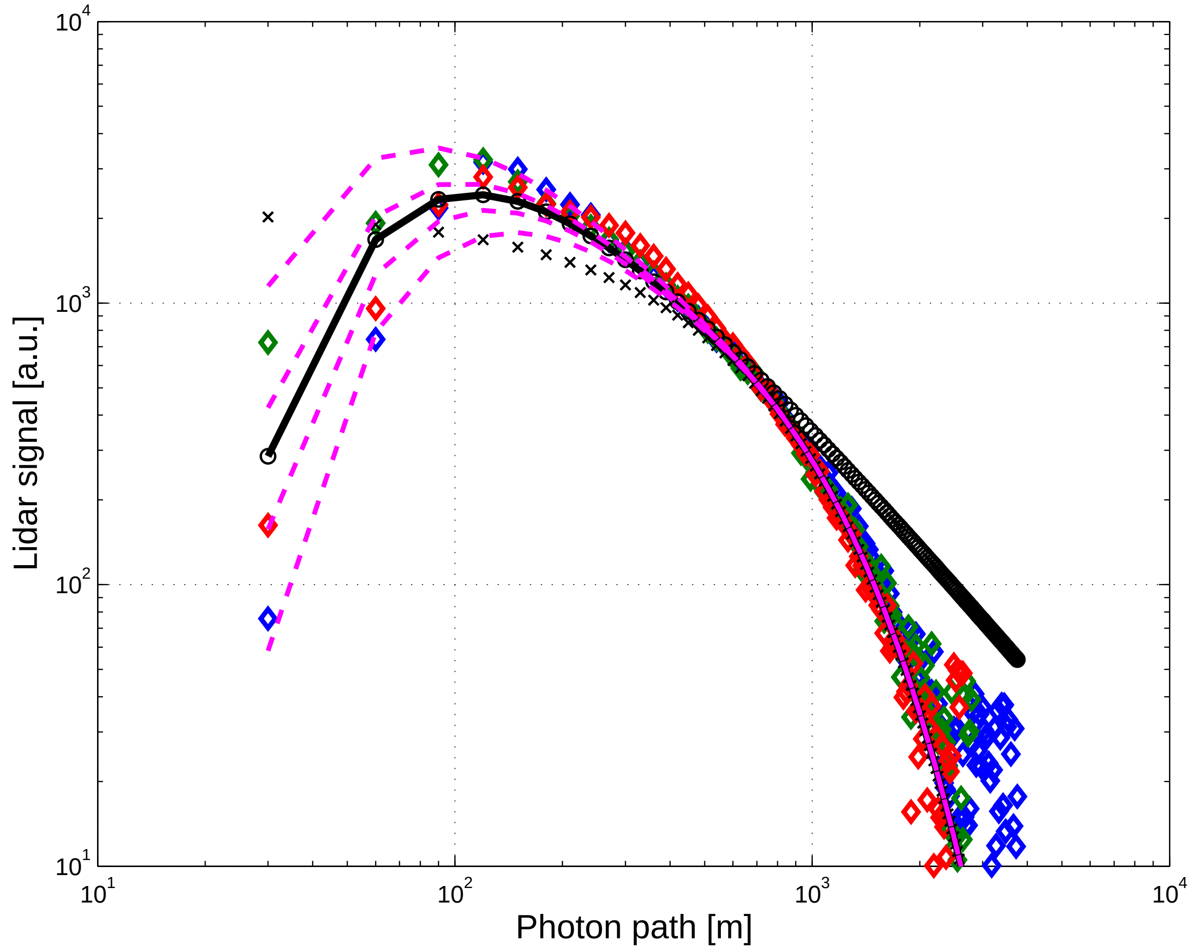

Fig. 1: Four LITE lidar returns as a function of sounding depth (open diamonds). The DA prediction is shown by a solid black line assuming $H = 252$ m and $(1-g)\sigma = 0.012\ m^{-1}$; hence, $\tau = \sigma H = 20.2$ for $g = 0.85$. Other choices of the parameters from Table 1 are in dashed lines. The first term of Eq. (23) is depicted by o-marks while the first term of Eq. (25) is shown by x-marks. The latter approximation is a reasonable model for the exponential tail of the pulses.

the latter expression better captures the exponential tail of the temporal Green function. The DA estimation made assuming $H = 252$ m and $(1-g)\sigma = 0.012$ m^{-1} is depicted by the black solid line. Assuming $g = 0.85$ as usual for water clouds, we estimate the optical depth $\tau = \sigma H$ to be ≈ 20.

Table 1: Parameters used in DA simulation of LITE pulses

case #	$\sigma(1-g)$ [m^{-1}]	H [m]
1	0.0167	230
2	0.0133	246
3	0.0123	252
4	0.0111	259
5	0.0095	270

Additional estimation with parameters enlisted in Table 1 is plotted by cyan-dashed lines. Within the framework of the DA, there is no way to separate the contribution of the extinction coefficient σ and the phase function asymmetry parameter g. The figure shows that the DA reasonably reproduces the shape of the lidar return pulse. The figure also shows that the first term of either Eq. (23) or of Eq. (25) cannot reproduce alone the observed shape of the lidar return in contrast to what can be observed in tissue optics. Additionally, Table 1 shows that the estimation of H can be done with rather high accuracy of ± 20 m which is 10% of 250 m. However, the accuracy of $(1-g)\sigma$ is not that good and is about 0.004 m^{-1} which is 30% of 0.0123 m^{-1}.

This uncertainty analysis is consistent with the conclusions of Devis et al. [7] who used the same data to estimate the first- and second-order moments of the in-cloud pathlength $\lambda = ct$ and compared them with the results of Monte Carlo simulations. Furthermore, the cloud parameters these authors would have inferred by using the homogeneous (rather than their preferred stratified) cloud model would be very similar to our present estimates. See their Fig. 3b reproduced here in our Fig. 2 and our discussion of it in the caption.

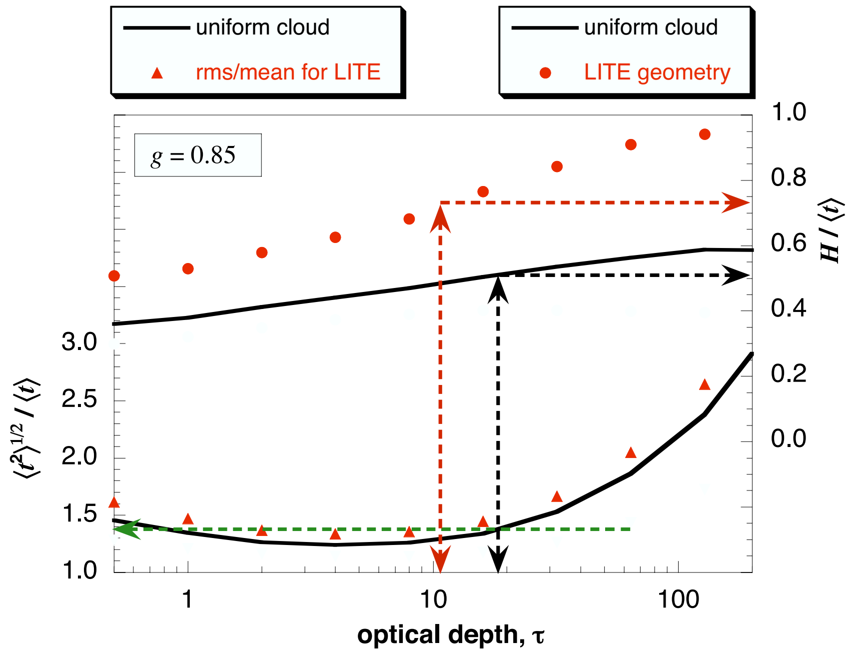

Fig. 2: Fig. 3b from Davis et al. [7] showing two step process for inferring cloud properties from the first and second moments of $\lambda = ct$, the in-cloud photon path, interpreting the observed LITE returns as a probability distribution. First, the ratio of the root-mean-square path to its mean is formed, ≈1.4, and used to seek an optical depth along the horizontal axis; the lower value is rejected because we know a priori that these clouds are quite opaque (data calibration would support this choice). Then the selected optical depth τ is used to find the proper ratio of the geometrical cloud thickness H to the mean path, $\approx$ 515 m; from there, H is inferred. Two cloud models are displayed: uniform structure (solid curves), and linear stratification of the extinction coefficient (symbols). The authors used the latter case to interpret the LITE data (dashed lines), leading to $\tau \approx 10$ and $H \approx 380$ m. The homogeneous slab model would lead to $\tau \approx 20$ and $H \approx 258$ m, in good agreement with the present estimates based on the fitting procedure in Fig. 1.

Appendix: The Poisson sum rule

A sum of the type

$$S = \sum_{n=-\infty}^{\infty} f(an+b), \tag{37}$$

where $f(x)$ is $L^{(2)}$ in the region $(-\infty, \infty)$ can be evaluated by the following process. If we define

$$f_+(x) = \begin{cases} 0; & x < 0, \\ f(x) & x > 0, \end{cases}, \tag{38}$$

$$f_-(x) = \begin{cases} f(x); & x < 0 \\ 0; & x > 0 \end{cases} \tag{39}$$

then

$$f_+(x) = \frac{1}{\sqrt{2\pi}} \int\limits_{-\infty+\mathrm{i}\tau_0}^{\infty+\mathrm{i}\tau_0} F_+(k)\mathrm{e}^{-\mathrm{i}kx}\mathrm{d}k. \tag{40}$$

Because of integrability of f, the constant τ_0 can be less than zero. Transform $F_+(k)$ is analytic for $\tau > \tau_0'$, $\tau_0 > \tau_0'$. We also have

$$f_-(x) = \frac{1}{\sqrt{2\pi}} \int\limits_{-\infty+\mathrm{i}\tau_1}^{\infty+\mathrm{i}\tau_1} F_-(k)\mathrm{e}^{-\mathrm{i}kx}\mathrm{d}k, \tag{41}$$

where $\tau_1 > 0$ and $F_+(k)$ are analytic for $\tau < \tau_1'$, $\tau_1 < \tau_1'$. Consider S as a sum of two parts:

$$S_+ = \sum_{n=0}^{\infty} f_+(an+b) = \frac{1}{\sqrt{2\pi}} \sum_{n=0}^{\infty} \int\limits_{-\infty+\mathrm{i}\tau_0}^{\infty+\mathrm{i}\tau_0} F_+(k)\mathrm{e}^{-\mathrm{i}k(an+b)}\mathrm{d}k, \tag{42}$$

$$S_- = \sum_{n=-\infty}^{-1} f_-(an+b) = \frac{1}{\sqrt{2\pi}} \sum_{n=-\infty}^{-1} \int\limits_{-\infty+\mathrm{i}\tau_1}^{\infty+\mathrm{i}\tau_1} F_-(k)\mathrm{e}^{-\mathrm{i}k(an+b)}\mathrm{d}k. \tag{43}$$

Because of absolute convergence of integrals, we can exchange sum and integral which results in

$$S_+ = \frac{1}{\sqrt{2\pi}} \int\limits_{-\infty+\mathrm{i}\tau_0}^{\infty+\mathrm{i}\tau_0} \frac{F_+(k)\mathrm{e}^{-\mathrm{i}kb}}{1-\mathrm{e}^{-\mathrm{i}ka}} \mathrm{d}k, \tag{44}$$

$$S_- = \frac{1}{\sqrt{2\pi}} \int\limits_{-\infty+\mathrm{i}\tau_1}^{\infty+\mathrm{i}\tau_1} \frac{F_-(k)\mathrm{e}^{\mathrm{i}ka-ikb}}{1-\mathrm{e}^{\mathrm{i}ka}} \mathrm{d}k. \tag{45}$$

The integrals can be evaluated using Cauchy's integral formula; the poles occur at zeros of denominator at $k = \frac{2\pi m}{a}$ where m is any positive or negative integer.

$$S_+ = \frac{\sqrt{2\pi}}{a} \sum_{m=-\infty}^{\infty} F_+(\frac{2\pi m}{a})\mathrm{e}^{-\mathrm{i}\frac{2\pi mb}{a}}, \tag{46}$$

$$S_- = \frac{\sqrt{2\pi}}{a} \sum_{m=-\infty}^{\infty} F_-(\frac{2\pi m}{a})\mathrm{e}^{-\mathrm{i}\frac{2\pi mb}{a}}. \tag{47}$$

Finally, we have the Poisson sum rule

$$S = \frac{\sqrt{2\pi}}{a} \sum_{m=-\infty}^{\infty} \mathrm{e}^{-\mathrm{i}\frac{2\pi mb}{a}} F\left(\frac{2\pi m}{a}\right). \tag{48}$$

References

[1] Davis, A. B., R. F. Cahalan, J. D. Spinhirne, M. J. McGill, and S. P. Love, "Off-Beam Lidar: An Emerging Technique in Cloud Remote Sensing Based on Radiative Green-Function Theory in the Diffusion Domain," *Phys. Chem. Earth*, **B24**, pp. 757–765, 1999.

[2] Zege, E. P., A. P. Ivanov, and I. L. Katsev, *Image Transfer Through a Scattering Medium* (Springer-Verlag, Heidelberg, 1991).

[3] Erdelyi, A., Ed., *Tables of Integral Transforms* (McGraw-Hill Book Company, Inc., USA, 1954)

[4] Marshak, A., A. Davis, W. J. Wiscombe, and R. F. Cahalan, "Radiative smoothing in fractal clouds," *J. Geophys. Res.*, **100**, pp. 26,247–26,261, 1995.

[5] Polonsky, I. N., S. P. Love, and A. B. Davis, "Wide-Angle Imaging Lidar (WAIL) Deployment at the ARM Southern Great Plains Site: Intercomparison of Cloud Property Retrievals," Los Alamos National Laboratory document LA-UR-03-9312 (to be published in *J. Atmos. and Oceanic Tech.*, **22**, 2005.)

[6] Winker, D. M., R. H. Couch, and M. P. McCormick, 1996: An Overview of LITE: NASA's Lidar In-Space Technology Experiment, *Proc. IEEE*, **84**, 164–180.

[7] Davis, A. B., D. M. Winker, and M. A. Vaughan, "First Retrievals of Dense Cloud Properties from Off-Beam/Multiple-Scattering Lidar Data Collected in Space," in *Laser Remote Sensing of the Atmosphere: Selected Papers from the 20th International Conference on Laser Radar, Vichy (France), July 9-14, 2000*, A. Dabas, C. Loth, and J. Pelon (Eds.) (Editions de l'Ecole Polytechnique, Palaiseau (France) 2001), pp. 35–38.